First-principles study of hydrogen ordering in β-YH_{2+x}

Sheng N. Sun, Yan Wang, and M. Y. Chou
School of Physics, Georgia Institute of Technology, Atlanta, Georgia 30332
(Received 2 August 1993)

The phase stability is studied for the β-phase YH_{2+x} system based on first-principles total energy calculations. Our study predicts that the $D0_{22}$, "40", and $D1_a$ structures are stable near $x=0.25$, 0.5, and 0.8, respectively. Using the effective cluster interactions obtained from the first-principles total-energy data, the phase diagram for the $D0_{22}$ and "40" ordered phases is calculated by the cluster variational method. The calculated order-disorder transition temperature at $x=0.1$ for the $D0_{22}$ structure is around 280 K, which is consistent with the recent observation of the metal-semiconductor transition near 230–280 K and resistivity anomalies near 200–250 K for the system with x near 0.1 [Daou and Vajda, Phys. Rev. B **45**, 10 907 (1992)].

I. INTRODUCTION

Hydrogen readily dissolves into many transition and rare-earth metals to form metal hydrides. Some super-stoichiometric metal dihydrides, expressed as MH_{2+x}, form interesting systems due to the sensitive dependence of their physical properties on x.[1,2] A large collection of metal dihydrides, MH_2, crystallizes in the CaF_2 structure. The metal atoms form a face-centered-cubic (fcc) structure with all the tetrahedral sites occupied by H. The x excess H, which occupies the octahedral sites, was found to play an important role in determining the magnetic, transport and structural properties of the system.[1–3] Unusual metal-semiconductor (MS) transitions have been found in CeH_{2+x} ($0.75 \le x \le 0.8$, 200–240 K) and LaH_{2+x} ($0.8 \le x \le 0.9$, 200–260 K) and were ascribed to the formation of a superlattice of octahedral vacancies below the transition temperature.[4] The recent experiment on the resistivity of the YH_{2+x} system by Daou and Vajda[1] also showed that the system (for $x \sim 0.1$) undergoes an interesting MS phase transition in the region 230–280 K, and it was speculated that the observed MS transition is driven by an order-disorder transition of octahedral hydrogen between 200–250 K determined by resistivity anomalies. Therefore, an investigation of the ordering possibility of octahedral hydrogen is important for the understanding of the MS transitions in the system.

The spatial distribution of the octahedral H may have a long-range order at low temperatures, i.e., form some kinds of superlattices. Despite of the great interest, the direct measurement of hydrogen ordering is still very limited; hydrogen orderings have only been confirmed for a few systems. A recent neutron-scattering study of TbD_{2+x} ($0.1 \le x \le 0.2$) showed positive signs of a $TiAl_3$-type ordering[3] (structurbericht symbol $D0_{22}$ or space-group notation $I4/mmm$), which can be characterized by the ordering of (420) planes where every fourth (420) plane is occupied by hydrogen. Both NiMo and Ni_4Mo-type orderings, where every other (for NiMo at $x=0.5$) and every fifth (for Ni_4Mo at $x=0.8$) (420) planes are empty, have been observed in the PdD_x system[5] and the latter structure was also suggested for the LaH_{2+x} system.[6] These experiments suggest that (420)-plane orderings are likely to be important in similar systems and deserve special attention. For the YH_{2+x} system, no experimental measurements of H ordering are available yet, and therefore it is not known if the octahedral hydrogen orders and what the ordered structure would be. It is tempting to expect that certain (420)-plane ordering occurs in the YH_{2+x} system because of the similarities in the electronic structure among some of the systems.

In this work, we investigate the possibility of octahedral hydrogen ordering in YH_{2+x} and, more importantly, calculate the x-T phase diagram for the identified ground state structures. The phase diagram study has been a major subject of research in the areas of metallurgy and condensed matter physics. In particular, the x-T phase diagram is of vital importance for the applications of alloys. The most recent development in these studies is to obtain the energetics of different structures from quantum mechanical electronic structure calculations. Then, the ground-state phase stability analysis can be done by comparing the formation energies of a group of ground-state candidates. Because searching through the 2^N possible states of an N-site lattice system is a formidable task computationally, one has to limit the search by defining a search set, which contains a subset of the 2^N structures. The most ambitious effort up to date in *ab initio* stability analysis used search sets of the order of ten $O(10)$ structures.[7,8] Though the results of the study can depend on the choice of the search set, the approach is, in general, successful when care is taken in selecting the structures in the search set.[7]

The phase-transition calculation requires the knowledge of the free energy of the system. Constructing a free-energy functional from the cluster expansion[9,10] provides a convenient way to treat the finite-temperature properties of an Ising system. Both the energy and entropy can be expanded in terms of the cluster functions.[9] In practice the expansion has to be truncated, but systematic improvement of calculations is possible, at least in principle. The method has been used to study the oxygen ordering in the high-T_c superconducting material[11] and the hydrogen ordering on metal surfaces[12] with empirical energy parameters. However, in this paper, we will use a

series of total-energy calculations to determine the parameters in the energy expansion. The latter approach has been successfully applied to many systems such as metal and semiconductor alloys.[7,8,13]

We applied this method to the study of the phase diagram in the hydrogen-metal system. A phase stability analysis of eleven ordered structures of the octahedral hydrogen in β-phase YH_{2+x} was first performed based upon first-principles calculations. Among the structures investigated, we found that the $D0_{22}$, "40", and $D1_a$ structures are the lowest-energy ordered states at $x=0.25$, $x=0.5$, and $x=0.8$, respectively. (Refer to Fig. 1 for the group symmetries of these structures.) Using the free energy constructed from the cluster expansion and the first-principle total-energy data, the order-disorder phase transitions for both the $D0_{22}$ and "40" structures are calculated by the cluster variational method (CVM).[10,14,15] Our study provides a theoretical prediction of the $D0_{22}$, "40", and $D1_a$ orderings in the system. The $D0_{22}$ ordering deserves special attention because it has been observed in a similar system, TbD_{2+x}. Our calculation for YH_{2+x} shows that the order-disorder transition temperature of the $D0_{22}$ structure at $x=0.1$ is around 280 K. This is in agreement with the recently observed MS transition near 230–280 K and resistivity anomalies near 200–250 K for the system with x near 0.1.[1] Our study not only supports the existence of octahedral H ordering, but also identifies the structure of the ordering and provides an absolute phase diagram for the system.

It is known that as x is increased to beyond 0.1, YH_{2+x} will go through a structural change from the pure β phase with metal atoms in the fcc structure to a mixture of the fcc and the hexagonal close-packed (the γ-phase) structures.[1,16] In this paper, we focus on identifying the possible ordered structures in the β phase and consider only the fcc-based superlattice structures. A comprehensive study of the system should take into account the contribution from both the fcc and hcp phases to the free energy of the system. At present, our study ignores the presence of the γ phase and hence the structural change of metal atoms.

II. FORMATION ENERGY AND STABLE PHASES

The self-consistent total-energy calculations are performed using *ab initio* pseudo potentials within the local-density-functional formalism[17] with Wigner correlation.[18] To represent the (pseudo) wave functions of any shape, we choose to use the plane-wave basis which is complete, orthogonal, and has the advantages of simplifying the calculation considerably. Soft pseudopotentials are generated for both yttrium and hydrogen atoms following the work by Troullier and Martins.[19] The true $1/r$ ionic hydrogen potential, which has poor convergence behavior is replaced by a pseudopotential in our calculation. The computational methods were tested by studying the structural properties of elemental yttrium and the results are in very good agreement with experiments.[20] A small energy cutoff of 36 Ry was found to achieve good convergence, which has made it feasible to carry out a number of supercell calculations for YH_{2+x}. It was also found that a correction in the exchange-correlation functional is needed to treat the outer core contribution in this early transition metal and the details of this has been presented elsewhere.[20] In our calculation, the Gaussian smearing method[21] was employed to accelerate the convergence of the total energy with respect to the number of k points. The number of plane waves included ranged from 900 to 7000 depending on the hydrogen concentration as well as the specific ordered structure involved. An iterative approach[22] was used to solve the eigenvalue problem. When self-consistency is achieved, which usually takes 4–6 iterations, the total energy is stable within at least 10^{-5} Ry per cell.

Name	FCC	D1	$D1_a$	$D0_{22}$	$L1_2$	$L1_0$	"40"
(100) Projection					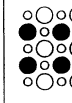	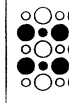	
Space Group: Int. Table	$Fm\bar{3}m$	$Fm\bar{3}m$	I4/m	I4/mmm	$Pm\bar{3}m$	P4/mmm	$I4_1/amd$
Schoenflies	O_h^5	O_h^5	C_{4h}^5	D_{4h}^{17}	O_h^1	D_{4h}^1	D_{4h}^{19}
Group No.	225	225	87	139	221	123	141
Formula	B	AB_7	AB_4	AB_3	AB_3	AB	A_2B_2

FIG. 1. The (100) plane projection of the seven superlattice structures of the octahedral hydrogen. The large circles represent the top (100) plane sites and the small circles represent the sites of the adjacent plane, which is shifted by $a/2$ relative to the top plane. Solid and hollow circles are the occupied and empty sites, respectively. All structures, except D1, are invariant under the translation of a in the (100) direction. The D1 structure, represented by the hatched circles, has a translational periodicity of $2a$ in the (100) direction. The complete hatched circles represent that the occupation by H is on the top (100) planes and the center hatched circles represent the occupation by H is on the plane shifted away from the top plane in the (100) direction by a. Some structures are associated with dual superlattices of both YH_{2+x} and $YH_{2+(1-x)}$.

Octahedral sites in the YH_{2+x} system also constitute a fcc lattice, which will be referred as the O-fcc lattice. The O-fcc lattice is shifted in space relative to the yttrium fcc lattice by $a/2$ in the (100) direction, where a is the lattice constant. Total energies, $E_{\rm tot}(V,\sigma)$, are calculated *ab initio* for eleven ordered structures in the O-fcc lattice as functions of volume V, where σ represents an ordered structure. The eleven structures include the fcc structure at $x=0$ and 1, the super fcc structure (or D1 in Ref. 7) at $x=0.125$, both the $L1_2$ and $D0_{22}$ structure at $x=0.25$ and 0.75, the $D1_a$ structures at $x=0.2$ and 0.8, and the $L1_0$ and the "40" structures at $x=0.5$. The seven different structures are shown in Fig. 1 together with their group symmetries. The total-energy data for each ordered structure are fitted to Murnaghan's equation of state,[23]

$$E_{\rm tot}(V)=E_0-\frac{BV_0}{B'}\left[\frac{(V/V_0)^{1-B'}-1}{1-B'}+\left[1-\frac{V}{V_0}\right]\right], \tag{1}$$

to extract equilibrium state properties and where V_0 is the equilibrium atomic volume, B is the bulk modulus, B' is the pressure derivative of the bulk modulus, and E_0 is the equilibrium total energy. In principle, one can search for the equilibrium volume numerically with numerous local-density-approximation (LDA) calculations and then calculate the total energy at that volume, but in practice this is computationally too expensive. Murnaghan's equation of state is very insensitive to B'; therefore we kept it fixed at 5.5 in our fitting. The calculated structural properties for the 11 ordered structures are summarized in Table I. Lattice contraction upon increasing octahedral hydrogen concentration was measured by x-ray diffraction and the contraction exists in a wide temperature range.[1] The calculated lattice constant (0 K) for YH_2 agrees with the experimental measurement (90 K) to within 0.2% and a clear lattice contraction upon increasing the octahedral hydrogen concentration is seen from the calculation. The electronic structure of the system shows that such a contraction is due to the maximization of the interactions of the hydrogen s and yttrium d orbitals at the octahedral sites. The detailed discussion on this will be presented elsewhere.[24]

To compare the relative stability of various ordered phases, we define the formation energy $\Delta E(\sigma)$ (following the work of Lu *et al.*[7] and Asta *et al.*[8] on metal alloys) as

$$\Delta E(\sigma,V)=E_{\rm tot}(\sigma,V)-xE_{\rm tot}(\bullet\text{-fcc},V)-(1-x)E_{\rm tot}(\circ\text{-fcc},V)\ , \tag{2}$$

where $E_{\rm tot}(\bullet\text{-fcc},V)$ and $E_{\rm tot}(\circ\text{-fcc},V)$ are the total energy of fcc structures with fully occupied and fully empty octahedral sites, respectively. The formation energy defined above is volume dependent. There exist different methods to use such information to treat lattice relaxation approximately.[13,25,26] In this paper, we adopt the approach that allows complete relaxation of individual ordered structures so that the absolute minimum formation energies of all the ordered structures are used to determine the effective interactions of the system. The effect of lattice relaxation will also be discussed in the next section.

The formation energy of a structure differs from the total energy by a shift in reference energy, which is the total energy of the constituents of the structure. As a result of this, a large constant contribution to the total energies is subtracted out in calculating the formation energies. This becomes obvious when one realizes that the total energies are in the order of 10^2 eV, whereas the formation energies are in the order of 10^{-2} eV for our system. To ensure that the systematic error is properly canceled in the formation energy calculation, it is very important that the same convergence criteria and k-space sampling are used in all the total energy calculations. We maintained the same energy cutoff and approximately the same k-space sampling in all the total-energy calculations.

The formation energies for the eleven structures are listed in Table II and shown in Fig. 2 by circles. We will compare these formation energies with the formation energies predicted by the cluster expansion formula in Sec.

TABLE I. Structural and elastic properties of YH_{2+x} for the 11 ordered compounds. The equilibrium total energies, lattice constants and the bulk moduli are obtained from the Murnaghan's fitting.

Structure	x	E_0 (Ry)	a (Å)	B (10^{11}dyn/cm^2)
fcc	0	−7.0128	5.195	8.4
D1	0.125	−7.1572	5.188	9.3
$D1_a$	0.2	−7.2441	5.184	8.7
$D0_{22}$	0.25	−7.3024	5.184	8.7
$L1_2$	0.25	−7.3009	5.185	8.6
$L1_0$	0.5	−7.5899	5.174	9.1
"40"	0.5	−7.5903	5.172	9.4
$L1_2$	0.75	−7.8735	5.168	9.5
$D0_{22}$	0.75	−7.8740	5.168	9.0
$D1_a$	0.8	−7.9310	5.165	9.8
fcc	1.0	−8.1547	5.167	9.9

TABLE II. The formation energies based on the LDA calculations according to Eq. (2) and predicted by the cluster expansion, Eq. (4). Cluster sets a, b, and c, include clusters of {1,2,3,5,7,9,12}, {1,2,3,5,6,7,9,12}, and {1,2,3,4,5,6,7,9,12}, respectively (refer to Table III for cluster number assignments). The formation energies are given in meV.

Structures	LDA	a	b	c
fcc ($x=0$)	0.0	0.0	0.0	0.0
D1 ($x=0.125$)	−23.5	−25.7	−25.4	−26.0
$D1_a$ ($x=0.2$)	−40.4	−40.6	−40.4	−40.6
$D0_{22}$ ($x=0.25$)	−56.9	−53.7	−54.6	−53.1
$L1_2$ ($x=0.25$)	−35.9	−48.5	−47.5	−43.8
$L1_0$ ($x=0.5$)	−83.5	−81.8	−82.6	−82.3
"40" ($x=0.5$)	−89.4	−90.3	−89.9	−90.1
$L1_2$ ($x=0.75$)	−58.1	−48.5	−47.5	−51.4
$D0_{22}$ ($x=0.75$)	−65.2	−67.6	−68.5	−70.3
$D1_a$ ($x=0.8$)	−63.5	−62.8	−62.6	−62.1
fcc ($x=1$)	0.0	0.0	0.0	0.0

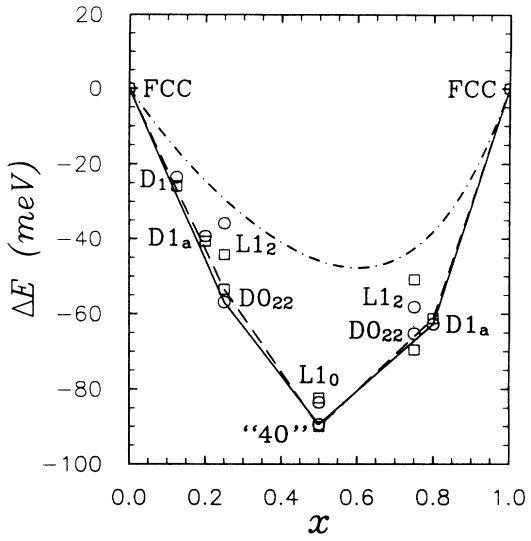

FIG. 2. The formation energies per YH_{2+x} calculated according to Eq. (2) for the 11 superlattice structures listed in Table I are shown in the figure by circles. The formation energies predicted by the cluster expansion using the ECI's of the set c in Table IV are shown by hollow squares. The three stable ordered structures according to the LDA calculations and the two fcc structures are connected with solid lines, which represent the lowest-energy states of the system, while the predicted formation energies for the same ground-state structures are connected by dashed lines. The predicted formation energy for the disordered phase is shown in a dot-dashed line.

IV. From this calculation, we can identify three structures, which have lower formation energies than that of the mixture of the neighboring structures. The three ground-state structures are the DO_{22} ($x=0.25$), the "40" ($x=0.5$), and $D1_a$ ($x=0.8$). A ground-state curve connecting the fcc ($x=0$ and 1) and the three stable ordered phases is shown in Fig. 2 (solid lines). Notice that the stable superstoichiometric structure with x closest to 0.1 when the MS transition is observed is the mixture of YH_2 and DO_{22} ordered $YH_{2.25}$, the latter is energetically much more favorable than the $L1_2$ structure. The formation energy difference between the DO_{22} and $L1_2$ structures is about 20 meV per YH_{2+x}. Both the super fcc structure at $x=0.125$ (D1 structure) and the $D1_a$ structure at $x=0.2$ are, however, unstable with respect to the heterogeneous mixture of the pure dihydride YH_2 and the DO_{22} ordered $YH_{2.25}$ by approximately 5 meV and 5.5 meV per YH_{2+x}, respectively. At higher concentrations, the LDA calculation shows that DO_{22} ($x=0.75$) is unstable with respect to the mixture of the "40" ($x=0.5$) and $D1_a$ ($x=0.8$) structures by only 2 meV. Since this is within the LDA uncertainty, the ground-state assignments at higher concentrations based on this study are not conclusive yet. Nevertheless, the study shows that the DO_{22} ordering at $x=0.25$ and possibly at $x=0.75$, the "40" ordering at $x=0.5$, and the $D1_a$ ordering at $x=0.8$ are possible for the fcc-based system. As will be shown later, our calculation gives the order-disorder transition temperature for the DO_{22} structure at $x=0.1$ around 280 K, which is very close to the temperature at which the MS transition and resistivity anomalies are observed for the system. A direct experimental observation of the ordering will be interesting and will also help establish the connection between the ordering and the MS transition.

III. CLUSTER EXPANSION AND FREE-ENERGY CONSTRUCTION

To study the finite-temperature properties of a system, the knowledge of the free energy for the system is required. A rigorous way to construct such a free-energy functional for an Ising system has been developed using the idea of cluster expansion[9,10,15] and been applied to several systems.[7,8,13] In the following, we will only outline the idea of the cluster expansion approach for clarity and to specify our notation. For details, the readers are directed to the references indicated above.

As a first-order approximation, the excess hydrogen can be thought as fixed at the octahedral sites which form the O-fcc lattice. The uncorrelated vibration of hydrogen around the equilibrium positions contributes equally to both the ordered and disordered phases at a given concentration and temperature and hence has no effect on the order-disorder phase transition. We ignore the contribution of the collective vibrational modes, which is not expected to be significant for low x. Therefore, only the configurational entropy is considered in this study.

The occupation of lattice sites by hydrogen can be described by an Ising model, which assigns a spin variable σ_i to each lattice site i. For this system, σ_i takes ± 1 depending upon whether the site is occupied or empty (or by the A or B species). Though the mapping of the microscopic configuration of hydrogen in a real host metal to the spin configuration of an Ising system is only an approximation because it ignores the relaxation of atoms completely, the Ising representation of the configuration is expected to work well for systems showing little lattice relaxation. The relaxation effect is important for systems where the atomic volume deference for two species is large.[13] However, the volume difference is not expected to be significant for our system due to the small size of hydrogen atoms. This is also supported by the fact that the equilibrium lattice constant changes less than 1% in the whole range of $0 \le x \le 1$. We use the fully relaxed total energy of each ordered compound in the formation energy calculation. This corresponds to the local relaxation scheme used by Wei *et al.*[13] and Sanchez and coworkers.[26]

In cluster expansion formalism, an arbitrary function of microscopic configuration, σ, can be expanded in terms of a complete set of orthogonal basis functions exactly. The basis function, defined as the products of spin variables, is also called the cluster function. Expanding the total energy per site (this also equals to the total energy per YH_{2+x} in our calculation), which is a function of microscopic spin configuration and of volume, we have[7]

$$e_{\rm tot}(\sigma,V)=\frac{1}{N}E_{\rm tot}(\sigma,V)=\sum_{\alpha} z_\alpha E_\alpha(V)\phi_\alpha(\sigma)\ , \qquad (3)$$

where $E_\alpha(v)$ is the effective cluster interaction (ECI), ϕ_α is the average of all the cluster functions related by group symmetries, and $z_\alpha = N_\alpha/N$ is the number of the α-type clusters per site. Using the definition of Eq. (2), the formation energy per site is given by

$$\Delta e(\sigma, V) = \sum_\alpha z_\alpha E_\alpha(V)[\phi_\alpha(\sigma) - \eta_\alpha(x)] , \tag{4}$$

where $\eta_\alpha(x) = x\phi_\alpha(\bullet\text{-fcc}) + (1-x)\phi_\alpha(\circ\text{-fcc})$. It is easy to verify that $\eta_\alpha(x) = 1$ for clusters of even sites and $\eta_\alpha(x) = 2x - 1$ for clusters of odd sites. In particular, Eq. (4) guarantees that the formation energies for the fcc structures are identically zero. It is also interesting to notice that the empty and single site clusters do not contribute to the formation energy according to Eq. (4). Therefore, the leading term in the expansion for the formation energy is the nearest-neighbor pair cluster.

Despite of the simplification due to group symmetry, in practice, one still has to assume that the ECI's *converge* rapidly with respect to the size of the clusters so that only a small number of terms need to be retained in Eq. (3). In fact, this is assumed in all relevant work to date. The truncated expansion of Eq. (3),

$$e_{\text{tot}}(\sigma, V) \approx \sum_\alpha^n z_\alpha E_\alpha(V)\phi_\alpha(\sigma) , \tag{5}$$

gives an approximate representation for the energetics of the system, where n is the number of reduced clusters retained in the expansion. To the extent that Eq. (5) is converged, it can be used to calculate the total energies of *any* phases, including the completely disordered phase. The reduced cluster function, $\phi_\alpha(\sigma)$, for the 11 ordered structures and all the clusters considered in this study, the degenerate factor z_α, and the structural weight factor ω (defined shortly) are summarized in Table III.

The ECI's can be calculated by directly inverting the expansion of Eq. (5) and this requires that the truncated basis vectors, $\phi_\alpha(\sigma)$ for $\alpha = 1,2,\ldots,n$, are linearly independent.[27] In general, the linear independence of $\phi_\alpha(\sigma)$ in a subspace due to truncation is not guaranteed by the orthogonality property of $\phi_\alpha(\sigma)$ in the whole space, therefore one must choose appropriate configurations to ensure that the inversion of Eq. (5) exists. This approach introduces a stronger dependence of the ECI's on the ordered structures chosen for the calculation and, hence, the nonuniqueness of the ECI's. In fact, sometimes the nonuniqueness of the ECI's still represents a problem that has not been solved satisfactorily to date. An alternative approach was suggested by Lu *et al.*[7] to reduce the dependence of the ECI's on the choice of ordered structures. The idea is to first calculate a larger pool of $\Delta E(\sigma)$ so that the ECI's can be determined by a least-squares minimization of the χ function, which is defined as

$$\chi^2 = \frac{1}{\sum_\sigma \omega_\sigma} \sum_\sigma \omega_\sigma \left[\Delta e(\sigma, V) - \sum_\alpha^n z_\alpha E_\alpha(V)[\phi_\alpha(\sigma) - \eta_\alpha(x)] \right]^2 , \tag{6}$$

where the structural weight ω_σ is determined by

$$\omega_\sigma = 48 N_c(\sigma)/N_G(\sigma) \tag{7}$$

for the fcc lattice. Here, $N_c(\sigma)$ and $N_G(\sigma)$ are the number of atoms per unit cell and the number of point-group operations for the ordered structure σ, respectively. The least-squares minimization method may reduce the dependence of the ECI's on the choice of ordered structures. For the CVM calculation a set of ECI's that is convergent and minimizes the χ function should be searched.

TABLE III. The reduced cluster function, $\phi_\alpha(\sigma)$, for all the subclusters of the tetrahedron-octahedron approximation and the third-neighbor pair cluster. The octahedral hydrogen concentration x is also used to distinguish the dual superlattice structures of the same symmetry, such as the $D0_{22}$ structure at $x = 0.25$ and 0.75. Clusters of number 1–12 are the empty, the point, the nearest-neighbor (NN) pair, the equilateral NN triangle, the equilateral NN tetrahedron, the second-nearest-neighbor (SNN) pair, the isosceles triangle of one SNN and two NN bonds, the square of four NN bonds, the nonequilateral tetrahedron of five NN and one SNN bonds, the pyramid of eight NN bonds, the octahedron, and the third-nearest-neighbor (TNN) pair cluster, respectively.

Structure	x	ω	$\phi_\alpha(\sigma)$											
			1	2	3	4	5	6	7	8	9	10	11	12
z_α			1	1	6	8	2	3	12	3	12	6	1	12
fcc	0	1	1	−1	1	−1	1	1	−1	1	1	−1	1	1
fcc	1	1	1	1	1	1	1	1	1	1	1	1	1	1
D1	$\frac{1}{8}$	8	1	$-\frac{3}{4}$	$\frac{1}{2}$	$-\frac{1}{4}$	0	$\frac{1}{2}$	$-\frac{1}{4}$	0	$-\frac{1}{2}$	$\frac{1}{4}$	$-\frac{1}{2}$	$\frac{1}{2}$
$D1_a$	$\frac{1}{5}$	30	1	$-\frac{3}{5}$	$\frac{1}{5}$	$\frac{1}{5}$	$-\frac{3}{5}$	$\frac{7}{15}$	$-\frac{1}{15}$	$-\frac{1}{15}$	$-\frac{1}{3}$	$\frac{7}{15}$	$-\frac{3}{5}$	$\frac{7}{15}$
$D1_a$	$\frac{4}{5}$	30	1	$\frac{3}{5}$	$\frac{1}{5}$	$-\frac{1}{5}$	$-\frac{3}{5}$	$\frac{7}{15}$	$\frac{1}{15}$	$-\frac{1}{15}$	$-\frac{1}{3}$	$-\frac{7}{15}$	$-\frac{3}{5}$	$\frac{7}{15}$
$D0_{22}$	$\frac{1}{4}$	12	1	$-\frac{1}{2}$	0	$\frac{1}{2}$	−1	$\frac{2}{3}$	$-\frac{1}{6}$	$\frac{1}{3}$	$-\frac{1}{3}$	$\frac{1}{6}$	0	$\frac{1}{3}$
$D0_{22}$	$\frac{3}{4}$	12	1	$\frac{1}{2}$	0	$-\frac{1}{2}$	−1	$\frac{2}{3}$	$\frac{1}{6}$	$\frac{1}{3}$	$-\frac{1}{3}$	$-\frac{1}{6}$	0	$\frac{1}{3}$
$L1_2$	$\frac{1}{4}$	4	1	$-\frac{1}{2}$	0	$\frac{1}{2}$	−1	1	$-\frac{1}{2}$	1	0	$-\frac{1}{2}$	1	0
$L1_2$	$\frac{3}{4}$	4	1	$\frac{1}{2}$	0	$-\frac{1}{2}$	−1	1	$\frac{1}{2}$	1	0	$\frac{1}{2}$	1	0
$L1_0$	$\frac{1}{2}$	6	1	0	$-\frac{1}{3}$	0	1	1	0	1	$-\frac{1}{3}$	0	1	$-\frac{1}{3}$
"40"	$\frac{1}{2}$	12	1	0	$-\frac{1}{3}$	0	1	$\frac{1}{3}$	0	$-\frac{1}{3}$	$\frac{1}{3}$	0	-1	$\frac{1}{3}$

Once a set of ECI's is obtained, one has an approximate expression for the energy of the system and it depends on the microscopic state of the system. The macroscopic quantity can be obtained as the ensemble average of the corresponding microscopic quantity and the ensemble average of the reduced cluster functions are defined as the correlation functions for the clusters. We denote the correlation functions as ξ_α. The free-energy per lattice site in the CVM can be written as

$$f(V,T,\xi_\alpha)=\sum_\alpha z_\alpha E_\alpha(V)\xi_\alpha - k_B T \sum_\alpha \gamma_\alpha \sum_J y_\alpha(J)\ln y_\alpha(J) , \quad (8)$$

where the first term is the parameterized total energy and the second term is the entropy expression from the CVM. Here k_B is the Boltzmann constant and T is the absolute temperature. In Eq. (8) γ_α is the Kikuchi-Baker coefficients, which is related to the symmetry of the lattice and can be calculated recursively.[14,15] The cluster probability $y_\alpha(J)$, where J represents a microscopic configuration of the cluster, can be expressed in terms of the correlation function ξ_α linearly as is shown by Sanchez and de Fontaine.[15] The phase diagram can be calculated by either the common tangent construction[28] from free energies or by searching for the intersection of the grand potentials for the ordered and disordered states directly at a given temperature.[29] The grand potential per site is defined as

$$g=f-\mu x , \quad (9)$$

where μ is the chemical potential and x is the octahedral hydrogen concentration. We used the grand potential method in our phase diagram calculation and treated the entropy term in Eq. (8) by the tetrahedron-octahedron (TO) truncation scheme.[15] The number of independent correlation functions in the TO approximation is 45 for the $D0_{22}$ structure[30] and 53 for the "40" structure when the point-group symmetries are taken into account. In solving for the equilibrium state, one has to minimize a thermodynamic function with respect to all the correlation functions ξ_α.

In our study, we found that considering only clusters within the TO approximation is not enough to ensure a converged energy expansion. It is very important to include the *third*-nearest-neighbor interaction in the energy expansion and the fitting shows that the third-nearest-neighbor interaction is much stronger than the multisite interactions. This will be discussed in more detail in the next section. To treat the cluster beyond the TO approximation in the energy term, we use the approach suggested by Carlsson[31] and Ferreira, Wei, and Zunger.[32] For a pair cluster, the approximation allows of a representation of the pair-correlation function by the product of two single-site correlation functions. Such an approximation scheme has also been used in a previous metal-alloy study.[8]

IV. CALCULATION OF THE EFFECTIVE CLUSTER INTERACTIONS

Apart from the truncation of the cluster expansion of entropy, there are two other sources of errors in the phase diagram calculation by the approach discussed in this paper. It is obvious that the relative uncertainties in the LDA energies (resulting from the pseudopotential approximation, plane-wave and k-point convergence, etc.) set a limit to the accuracy of the phase diagram. It is estimated to be about 2–3 meV, which corresponds to 20–30 K. The second source of error is due to the ECI parameterization of the energy, which can introduce a larger error than the LDA calculation. Therefore, it is ideal to improve the parameterization systematically to make these two errors comparable.

As discussed earlier in the paper, the (420)-plane orderings are important in the metal hydride systems and several of them have indeed been observed experimentally. Our first-principles calculation shows that the $D0_{22}$ structure, a (420)-plane ordering, is much more stable than the $L1_2$ structure for $YH_{2.25}$. An interesting question to ask is then what kinds of interaction are likely to be important for these orderings? By examining the $D0_{22}$ ($x=0.25$) and the $D1_a$ ($x=0.2$) structures, it can be seen that many octahedral hydrogen are connected by third-nearest-neighbor pair clusters. In fact, this is a crucial observation and the third-nearest-neighbor pair interaction indeed plays a very important role in the parameterization of the formation energies.

The temperature scale of the order-disorder transition, and, hence, the phase diagram is determined by the ordering energies (defined as the difference in the formation energies of the disordered and ordered states at zero K) of various structures. To obtain a phase diagram as accurately as possible, it is extremely important that a set of ECI's that is well converged and represents correctly the energetics of the system be used. We show how this is achieved in detail in this section. The absolute convergence of the ECI's with the increase of cluster sizes is, in general, hard to quantify because the "size" of a cluster is not well defined. For example, it is hard to argue that the forth-nearest-neighbor cluster is larger or smaller than the octahedron cluster. In practice, one can test the convergence of the ECI's by increasing the basis of the cluster expansion. For example, we can consider the expansion of the formation energy in terms of seven to nine clusters and examine the stability of some relevant physical quantities. A well-converged expansion should produce a minimal variation of relevant quantities.

In the cluster expansion of the formation energy, we consider all the clusters within the TO approximation and the third-nearest-neighbor (TNN) interaction. We use the least-squares fitting approach to determine a set of best ECI's from the 11 calculated formation energies. In these fittings, we require the participation of the nearest neighbor and the third-nearest-neighbor pair clusters and consider all the possible choices for the remaining cluster within the TO approximation. The best sets and the fitting errors, χ function, for the basis sets containing seven to nine clusters are listed in Table

TABLE IV. Convergence of the cluster expansion upon increasing the expansion basis is shown. Basis sets *a*, *b*, and *c*, include clusters of {1,2,3,5,7,9,12}, {1,2,3,5,6,7,9,12}, and {1,2,3,4,5,6,7,9,12}, respectively. The ECI's and the formation energies of the disordered state are given in meV.

Sets	χ	E_1	E_2	E_3	E_4	E_5	E_6	E_7	E_9	E_{12}	Δe_{dis} ($x=0.25$)	Δe_{dis} ($x=0.50$)	Δe_{dis} ($x=0.75$)
a	3.3			12.3		−3.2		1.7	1.0	−2.1	−34.4	−54.9	−50.0
b	3.3			13.3		−3.6	−2.4	1.7	1.3	−2.8	−29.4	−47.6	−45.0
c	3.0			13.5	0.5	−3.5	−2.6	1.2	1.3	−2.9	−29.8	−46.8	−43.5

IV. The purpose is to show the convergence upon increasing the basis of expansion. Since the phase diagram depends strongly on the ordering energies of different structures, a good test of convergence is to see how stable the energy of the disordered phase is as we increase the basis of expansion. The formation energies for the disordered phase at several concentrations are also shown in Table IV. It is clear that the cluster expansion is converging. The best fitting of nine clusters include the constant, the point, the nearest-neighbor (NN) pair, the equilateral NN triangle, the equilateral NN tetrahedron, the second-nearest-neighbor (SNN) pair, the isosceles triangle, the nonequilateral tetrahedron, and the TNN clusters. This particular fitting only introduces a χ function of 3 meV.

The predicted formation energies from the seven to nine cluster sets are listed in Table II for comparison with the values from the LDA calculations. The best predictions of the formation energies from the set *c* are also plotted in Fig. 2 (hollow squares). The predicted formation energies of the five ground-state ordered structures are connected by dashed lines. For a completely disordered state, the correlation functions for multisite clusters can be given by the product of the point-cluster correlations due to the statistical independence of each lattice site. The single-site correlation function, ξ_2, is related to the octahedral hydrogen concentration x by

$$x=\tfrac{1}{2}(1+\xi_2)\ . \tag{10}$$

Therefore, for a given set of ECI's, the formation energy of the disordered state as a function of x can be calculated according to

$$\Delta e_{dis}(x)=\sum_{\alpha} z_\alpha E_\alpha[(2x-1)^{t_\alpha}-\eta_\alpha(x)]\ , \tag{11}$$

where t_α is the number of lattice sites associated with the cluster α. The predicted formation energy for the disordered state is also shown in Fig. 2 by the dot-dashed line.

V. x-T PHASE DIAGRAM AND DISCUSSIONS

The ECI's from the nine cluster least-squares fitting represents the best set of effective interaction parameters achieved from our 11 LDA total-energy data base. The prediction of the formation energies by the cluster expansion formula with an error large than the LDA uncertainty occurs for the two $L1_2$ structures and the two $D0_{22}$ structures. This is due to the difficulties associated with fitting the large formation energy difference between the $L1_2$ and the $D0_{22}$ structures at the same concentration within the TO approximation and a third-neighbor cluster. It is known that the $L1_2$ and the $D0_{22}$ structures are degenerate within the tetrahedron approximation; the only clusters that are responsible for the formation energy difference are those beyond the tetrahedron approximation. In principle, the fitting can be improved by using a larger basis for the cluster expansion and performing more LDA calculations. For our limited LDA data base of 11 structures, the largest prediction error is about 8 meV for the $L1_2$ structure at $x=0.25$. For ground-state ordered structures, the largest prediction error is about 4 meV for the $D0_{22}$ structure at $x=0.25$. These errors are about two to three times the LDA error, but it represents the best can be achieved within this limited calculation.

The x-T phase diagram for the $D0_{22}$ ($x=0.25$) and the "40" ($x=0.5$) structures is calculated using the ECI's shown in Table IV (set *c*) and the phase diagram is shown in Fig. 3. The prediction of the transition temperature near $x=0.1$ is around 280 K. The experimentally observed MS transition temperature is between 230–280 K and resistivity anomalies between 200 and 250 K for the same system. Given the fact that the CVM calculation usually overestimates the transition temperature slightly,

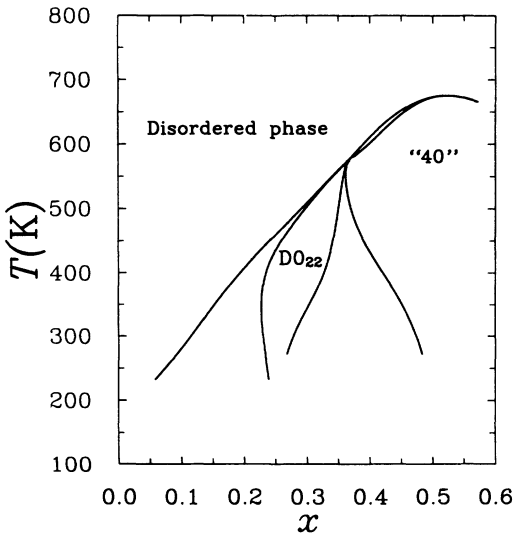

FIG. 3. The temperature-concentration order-disorder phase diagram is calculated for the $D0_{22}$ ($x=0.25$) and the "40" ($x=0.5$) structures using the ECI's of the set *c* in Table IV. The transition temperature at $x=0.1$ is around 280 K.

we thus conclude that the ordering of the octahedral hydrogen into a $D0_{22}$ structure is likely to be responsible for the resistivity transitions observed in these systems. A direct diffraction experiment of the $D0_{22}$ ordering in the system will be needed to confirm this.

There is a second MS transition observed in the YH_{2+x} system in the temperature region of 80 K.[1] This transition is, however, not related to the breakdown of any long-range order of hydrogen because of the reversal of the metal and semiconductor phases as a function of temperature. Daou and Vajda[1] have suggested that the localization of electrons due to the presence of atomic disorder at low temperatures is responsible for this transition, however, the true mechanism is still not fully understood.

There are many possible superlattice structures that we did not consider in this work and it is not clear if any of these will order at low temperatures. One can consider, for example, the (420)-plane orderings for $x=\frac{1}{6}$, $\frac{1}{7}$, or $\frac{1}{8}$, to name a few. In fact, the possibilities to construct ordered structures near a given concentration seem unlimited. Since a complete search through 2^N configurations is formidable, the experimental observations, when available, should be used as a guideline in selecting the search set. Nevertheless, these lower x ordered structures would represent greater computational challenges because relatively large supercells with low symmetries are required for the total-energy calculations. We are interested in investigating the phase stability of these low symmetry structures in the future work.

VI. CONCLUSION

In conclusion, we studied the phase stability of the fcc YH_{2+x} system by combining *ab initio* total-energy calculations with the phase diagram calculations using the cluster variational method. The approach represents a *parameter free* treatment of the phase transition of an ising-like system based upon quantum-mechanical total-energy calculations. The theory predicts not only the existence of the $D0_{22}$, "40", and $D1_a$ orderings near $x=0.25$, 0.5, and 0.8, but also the absolute phase diagram for the $D0_{22}$ and "40" structures. The calculation of the phase diagram for the $D1_a$ structure near $x=0.8$ is deferred because our LDA calculation cannot resolve if the $D0_{22}$ structure at $x=0.75$ is a ground state at the moment. The transition temperature of the $D0_{22}$ phase to the disordered phase occurs at 280 K for $x=0.1$, suggesting that the ordering may be responsible to the MS transition and resistivity anomalies observed in the same system.

ACKNOWLEDGMENTS

We thank Dr. Siqing Wei for very useful discussions on symmetry groups and cluster algebra. This research is supported by the U.S. Department of Energy under contract No. DE-FG05-90ER45431 and partly by the NFS. A grant for supercomputer time from the Pittsburgh Supercomputing Center is also acknowledged. M.Y.C. acknowledge the support of the Packard Foundation.

[1] J. N. Daou and P. Vajda, Phys. Rev. B **45**, 10907 (1992); P. Vajda and J. N. Daou, Phys. Rev. Lett. **66**, 3176 (1991).
[2] J. P. Burger, P. Vajda, and J. N. Daou, J. Phys. Chem. Solids **52**, 779 (1991); P. Vajda, J. P. Burger, and J. N. Daou, Europhys. Lett. **11**, 567 (1990).
[3] G. André, O. Blaschko, W. Schwarz, J. N. Daou, and P. Vajda, Phys. Rev. B **46**, 8644 (1992).
[4] J. Shinar, B. Dehner, R. G. Barnes, and B. J. Beaudry, Phys. Rev. Lett. **64**, 563 (1990); J. Shinar, B. Dehner, B. J. Beaudry, and D. T. Peterson, Phys. Rev. B **37**, 2066 (1988).
[5] O. Blaschko, Phys. Rev. B **29**, 5187 (1984); J. Less-Common Met. **100**, 307 (1984); T. E. Ellis, C. B. Satterthwaite, M. H. Mueler, and T. O. Brun, Phys. Rev. B **42**, 456 (1979).
[6] P. Klavins, R. N. Shelton, R. G. Barnes, and B. J. Beaudry, Phys. Rev. B **29**, 5349 (1984).
[7] Z. W. Lu, S-H. Wei, A. Zunger, S. Frota-Pessoa, and L. G. Ferreira, Phys. Rev. B **44**, 512 (1991).
[8] M. Asta, D. de Fontaine, M. van Schilfgaarde, M. Sluiter, and M. Methfessel, Phys. Rev. B **46**, 5055 (1992).
[9] J. M. Sanchez, F. Ducastelle, and D. Gratias, Physica **128A**, 334 (1984).
[10] R. Kikuchi, Phys. Rev. B **81**, 988 (1951).
[11] A. Berera and D. de Fontaine, Phys. Rev. B **39**, 6727 (1989); L. T. Wille, Phys. Rev. B **40**, 6931 (1989).
[12] S. N. Sun and M. Y. Chou, Surf. Sci. **280**, 415 (1993).
[13] S-H. Wei, A. A. Mbaye, L. G. Ferreira, and A. Zunger, Phys. Rev. B **36**, 4163 (1987); S-H. Wei, L. G. Ferreira, and A. Zunger, **41**, 8240 (1990).
[14] J. Hijmans and J. de Boer, Physica **21**, 471 (1955); **21**, 485 (1955); **21**, 499 (1955); J. A. Barker, Proc. R. Soc. London Ser. A **216**, 45 (1953).
[15] J. M. Sanchez and D. de Fontaine, Phys. Rev. B **17**, 2926 (1978).
[16] A. Pebler and W. E. Wallace, J. Phys. Chem. **66**, 148 (1962).
[17] P. Hohenberg and W. Kohn, Phys. Rev. **136**, B864 (1964); W. Kohn and L. J. Sham, **148**, A 1133 (1965).
[18] E. Wigner, Phys. Rev. **46**, 1002 (1934).
[19] N. Troullier and J. L. Martins, Phys. Rev. B **43**, 1993 (1991).
[20] Y. Wang and M. Y. Chou, Phys. Rev. B **44**, 10339 (1991).
[21] C. L. Fu and K. M. Ho, Phys. Rev. B **28**, 5480 (1983).
[22] D. M. Wood and A. Zunger, J. Phys. A **18**, 1343 (1985).
[23] F. D. Murnaghan, Proc. Natl. Acad. Sci. USA **30**, 244 (1944); O. L. Anderson, J. Phys. Chem. Solids **27**, 547 (1966).
[24] Y. Wang and M. Y. Chou (unpublished).
[25] M. Sluiter and P. E. A. Turchi, Phys. Rev. B **40**, 11215 (1989).
[26] J. M. Sanchez, J. P. Stark, and V. L. Moruzzi, Phys. Rev. B **44**, 5411 (1991); J. D. Becker, J. M. Sanchez, and J. K. Tien, in *High Temperature Intermetallic Alloys IV,* edited by L. A. Johnson, D. P. Pope, and J. D. Stiegler, MRS Symposia Proceedings No. 213 (Materials Research Society, Pittsburgh, 1991), p. 133.
[27] W. D. Connolly and A. R. Williams, Phys. Rev. B **27**, 5169

(1983).
[28]D. A. Porter and K. E. Easterling, *Phase Transformations in Metals and Alloys* (Van Nostrand Reinhold, London, 1987).
[29]R. Kikuchi, J. Phys. (Paris) Colloq. **38**, C7-307 (1977).
[30]J. M. Sanchez and D. de Fontaine, Phys. Rev. B **21**, 216 (1980).
[31]A. E. Carlsson, Phys. Rev. B **35**, 4858 (1987).
[32]L. G. Ferreira, S.-H. Wei, and A. Zunger, Phys. Rev. B **40**, 3197 (1989).